

Binding Characterization of GPCRs-Modulator by Molecular Complex Characterizing System (MCCS)

Zhiwei Feng,[§] Tianjian Liang,[§] Siyi Wang,[§] Maozi Chen, Tianling Hou, Jack Zhao, Hui Chen, Yuehan Zhou, and Xiang-Qun Xie^{*}



Cite This: <https://dx.doi.org/10.1021/acschemneuro.0c00457>



Read Online

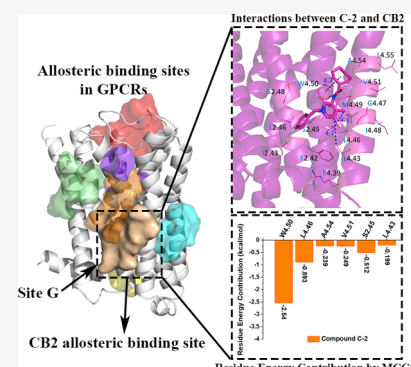
ACCESS |

Metrics & More

Article Recommendations

ABSTRACT: Increasing attention has been devoted to allosteric modulators as the preferred therapeutic agents for their colossal advantages such as higher selectivity, fewer side effects, and lower toxicity since they bind at allosteric sites that are topographically distinct from the classic orthosteric sites. However, the allosteric binding pockets are not conserved and there are no cogent methods to comprehensively characterize the features of allosteric sites with the binding of modulators. To overcome this limitation, our lab has developed a novel algorithm that can quantitatively characterize the receptor–ligand binding feature named Molecular Complex Characterizing System (MCCS). To illustrate the methodology and application of MCCS, we take G protein coupled receptors (GPCRs) as an example. First, we summarized and analyzed the reported allosteric binding pockets of class A GPCRs using MCCS. Sequentially, a systematic study was conducted between cannabinoid receptor type 1 (CB1) and its allosteric modulators, where we used MCCS to analyze the residue energy contribution and the interaction pattern. Finally, we validated the predicted allosteric binding site in CB2 via MCCS in combination with molecular dynamics (MD) simulation. Our results demonstrate that the MCCS program is advantageous in recapitulating the allosteric regulation pattern of class A GPCRs of the reported pockets as well as in predicting potential allosteric binding pockets. This MCCS program can serve as a valuable tool for the discovery of small-molecule allosteric modulators for class A GPCRs.

KEYWORDS: Allosteric modulator, MCCS, feature characterization, residue energy contribution, GPCRs



INTRODUCTION

G protein coupled receptors (GPCRs), also known as 7 transmembrane (7TM) domain receptors, represent the largest family of membrane proteins in the human genome. They trigger a variety of extracellular signal transduction pathways in response to stimuli such as hormones, neurotransmitters, growth and developmental factors, light, odors, and gustative molecules.¹ Their wide distribution in the human genome, engagement in essential physiological processes, and accessibility for small-molecule targeting make them a top class of therapeutic targets, associating with 30–40% of currently marketed drugs.² On the basis of the similarity and diversity of amino acid sequences and functions, GPCRs can usually be classified into five groups: Rhodopsin (class A), Secretin (class B1), Adhesion (class B2), Glutamate (class C), and Frizzled (class F).^{3,4} Among them, the class A GPCR family is the largest superfamily, which consists of four major groups with 13 sub-branches.⁵

Cannabinoid receptors, members of the class A GPCRs, are a part of the endocannabinoid system. Currently, there are two subtypes of cannabinoid receptors, including the cannabinoid receptor type 1 (CB1) and cannabinoid receptor type 2 (CB2). CB1 receptors are distributed mostly in the central nervous system (CNS). They influence a wide range of essential

physiological functions such as nociception, motor coordination, regulation of appetite, mood, and memory.⁶ On the contrary, CB2 receptors are mainly expressed in peripheral tissues such as the spleen, thymus, mast cells, and blood cells.^{7–9} Both CB1 and CB2 are involved in modulatory functions like immune system regulation, cell apoptosis, and migration.¹⁰ Thus, both cannabinoid receptors are promising targets for the development of small-molecule drugs.

Each GPCR has a distinctive ligand binding site or the so-called orthosteric binding site for the endogenous compound(s). Most of the FDA-approved drugs of GPCRs target the orthosteric binding sites. However, the orthosteric ligands have disadvantages such as poor efficacy, subtype selectivity, and potential of resistance. With an increasing number of drugs targeting the orthosteric sites being withdrawn from the market,

Received: July 20, 2020

Accepted: September 17, 2020

Published: September 17, 2020

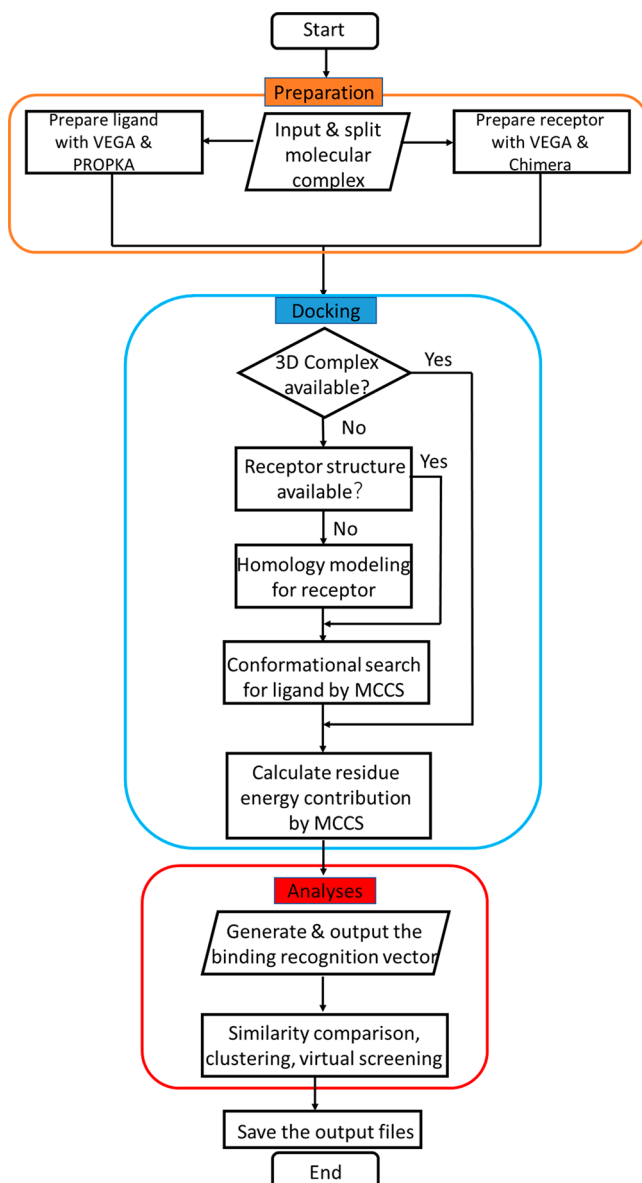


Figure 1. General workflow of MCCS. The major procedures of MCCS include (1) preparation, (2) docking and calculation, (3) analyses, and (4) final results.

considerable attention has been shifted to the discovery of the GPCRs allosteric modulators.¹¹

Allosteric regulation is the interaction between receptors and modulators, which is topographically distinguished from the orthosteric site of the protein. The binding of modulators at

the allosteric site often results in a conformational change of the receptor, which may affect the binding properties of orthosteric ligands. These modulations occur in one of the three following ways: (1) positive allosteric modulators (PAMs) that potentiated the response of protein to ligands; (2) negative allosteric modulators (NAMs) that decreased the ligand-mediated protein response; or (3) silent allosteric modulators (SAMs) that occupied the allosteric site blocking the action of PAMs or NAMs while inducing no functional effect. To date, a few allosteric modulators have already entered the market. For example, Cinacalcet (Sensipar), a PAM of the calcium-sensing receptor (CaSR), approved by the FDA in 2004, was the first allosteric GPCR modulator that entered the pharmaceutical market as a treatment for hyperparathyroidism¹² and Maraviroc (Selzentry), a NAM of chemokine CC-motif receptor 5 (CCR5), was approved in 2007 to treat patients infected with HIV.¹³

Unlike the conserved orthosteric sites, the allosteric binding pockets of GPCRs present higher divergence across subtypes of receptors from the same family. This mechanism allows for the potential of designing small molecules with ‘absolute subtype selectivity’. An additional advantage of allosteric regulation is that most of the modulators can only exert effects in the presence of the endogenous ligands. Thus, the allosteric modulators show both spatial and temporal selectivity. Last but not least, allosteric modulators lower the potential toxicity due to the “ceiling” effect. Because the allosteric modulators depend on the endogenous orthosteric ligand to exert their effect, the receptor activation will not surpass the ceiling defined by protein saturation even with an extremely high concentration of the potentiator.¹⁴

For the past two decades, innovative technologies such as X-ray crystallography and transmission electron cryo-microscopy (cryo-EM) enable the determination of an increasing number of 3D protein structures with high resolution. To date, a few GPCRs allosteric regulation patterns have been reported. In order to explore the detailed interaction pattern between GPCRs and allosteric modulators, we here systematically analyzed the key binding residues and their energy contributions on the basis of the reported 3D X-ray crystal or cryo-EM structures. Given the results, we further analyzed the allosteric binding site at CB1 and predicted the potential allosteric site for CB2 in the hope of facilitating the future design of novel modulators that target these two receptors.

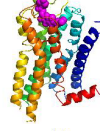
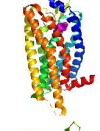
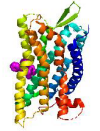
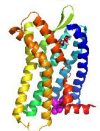
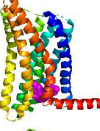
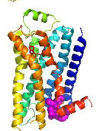
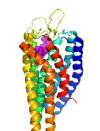
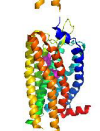
RESULTS AND DISCUSSION

Innovation of MCCS. In order to quantitatively describe the energy contribution of key residues involved in the binding sites of the receptor, we recently developed a Molecular Complex Characterizing System (MCCS), which will help to improve

Table 1. Different Terms of Residue Energy Contribution Based on the Reported 3D Crystal Structure ACM2 (kcal/mol)

residue	BW numbering	energy contribution	sum of steric components	sum of hydrophobic components	sum of hydrogen-bonding components
Trp422	7.35	-2.038	-1.549	-0.489	0
Tyr177	N/A	-1.555	-1.342	-0.212	0
Asn410	6.58	-0.665	-0.507	0	-0.158
Asn419	7.31	-0.566	-0.503	-0.063	0
Tyr83	2.63	-0.505	-0.398	-0.107	0
Tyr426	7.38	-0.397	-0.375	-0.022	0
Ile178	N/A	-0.333	-0.333	0	0
Tyr80	2.60	-0.324	+0.263	0	-0.587
Glu172	N/A	-0.265	-0.265	0	0
Cys176	N/A	-0.248	-0.248	0	0

Table 2. Summarization of All Reported Allosteric Regulation Structures^{48–50}

Site	Receptor	PDB code	Class/Branch	Structure	Reference
A	ACM2	4MQT	A/Alpha		⁴⁹
	PAR2	5NDD	A/Delta		⁴⁸
B	C5AR1	5O9H	A/Gamma		²⁰
	FFAR1	5TZY	A/Delta		²¹
C	CCR2	5T1A	A/Gamma		²³
	CCR9	5LWE	A/Gamma		²⁴
	ADRB2	5X7D	A/Alpha		²²
D	FFARI	4PHU	A/Delta		⁴⁹
	5TZR		A/Delta		²¹
E	PAR2	5NDZ	A/Delta		⁴⁸
F	P2Y1	4XNV	A/Delta		⁵⁰
G	CNR1	6KQI	A/Alpha		²⁷

the success rate of drug discovery.¹⁵ MCCS is open source under Apache License 2.0 and is freely available on GitHub at <https://github.com/stcmz/jdock/> and <https://github.com/stcmz/mccsx>. The features, applications, and step-by-step tutorials of MCCS can be found on GitHub. To improve the

automatic procedures, we have integrated many different programs or tools into MCCS, such as Chimera,¹⁶ VEGA,¹⁷ and PROPKA.¹⁸ MCCS has the ability of calculating residue energy contribution, the binding recognition vector, and vector similarity with reduced time-consumption and high accuracy.

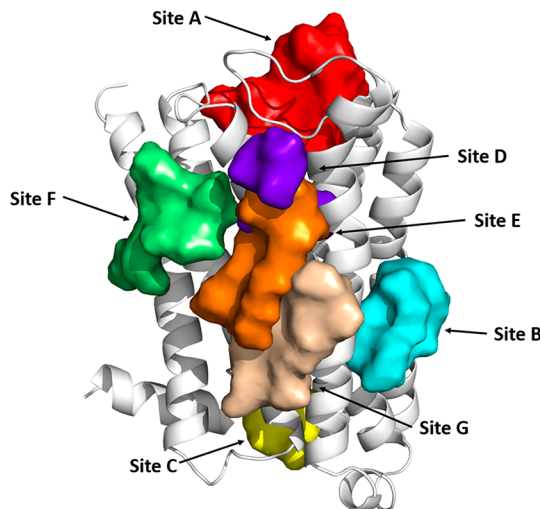


Figure 2. Summary of allosteric binding pockets of class A GPCRs. Seven allosteric binding pockets have been identified on the basis of the reported 11 PDB files.

Workflow of MCCS. The general procedure of MCCS is described in Figure 1. Briefly, (1) the input file of receptor or ligand is uploaded as the PDB file. (2) Then, MCCS is used to prepare and convert the PDB files to PDBQTs. (3) MCCS calculates the energy contribution of each residue involved in the binding site of reported protein–ligand complex. (4) Sequentially, a protein-sequence-based vector embedded with residue energy contribution is constructed to characterize the binding feature of a receptor and its ligand. (5) Finally, a reliable energy contribution vector is used to cluster similar ligands or proteins, select potential drug candidates during the virtual screening, and more. In the present work, we mainly focused on the calculation of residue energy contribution by MCCS.

Output Example of MCCS. Table 1 is the output example of the complex of human M2 muscarinic acetylcholine receptor (ACM2) bound to allosteric modulator LY2119620 (PDB: 4MQT).¹⁹ The total binding energy of the allosteric modulator LY2119620 in ACM2 was -9.790 kcal/mol, which was calculated from the sum of intraligand free energy (-0.119 kcal/mol)

and interligand free energy (-9.671 kcal/mol). The interligand free energy is the total energy of interacted atom pairs between the modulator (LY2119620) and the ACM2 receptor, which can be computed and further divided into the energy contribution of each residue. Moreover, each residue energy contribution can be further decomposed into (i) the “sum of steric components” that included gauss1, gauss2, and repulsion, (ii) the “sum of hydrophobic components”, and (iii) the “sum of hydrogen-bonding components”. Taking Trp422^{7,35} in ACM2 receptor as an example (Table 1), the total energy contribution of Trp422^{7,35} to the complex of LY2119620-ACM2 was -2.038 kcal/mol, which can be decomposed into (i) -1.549 kcal/mol from the “sum of steric components”, (ii) -0.489 kcal/mol from the “sum of hydrophobic components”, and (iii) 0 kcal/mol from the “sum of hydrogen-bonding components”. These different terms of residue energy contributions are listed in Table 1.

Reported Allosteric Binding Pockets of Class A GPCRs.

We summarized all 11 PDB files (Table 2) containing reported class A GPCRs (including α , δ , and γ sub-branches) with effective allosteric modulator–receptor interaction. As shown in Figure 2, a total of 7 allosteric binding regions have been identified. Though the crystallized protein–modulator complexes revealed multiple allosteric binding sites for class A GPCRs, three sites (Sites A, B, and C) are more typical than others; thus, we focused our discussion on these regions in this section. Of course, due to the limited number of reported structures, the conclusion in the following studies for each allosteric binding site of a receptor may only indicate a degree of binding feature of its receptor–modulator complex.

As shown in Figure 2, Site A (allosteric pocket) locates in the extracellular vestibule, which is surrounded by the second extracellular loop (ECL2) and the upper part of the orthosteric binding region in class A GPCRs. Muscarinic acetylcholine receptor M2 (ACM2) is a typical receptor with an allosteric binding region that located in this extracellular vestibule. To further investigate allosteric interactions in Site A, we applied our newly developed program MCCS to analyze the small-molecule-receptor recognition pattern based on the cocrystal structure of ACM2 (PDB: 4MQT).¹⁹ As shown in Figure 3, we found that Trp422^{7,35}, Tyr177^{ECL2}, Asn410^{6,58}, Tyr83^{2,64}, and

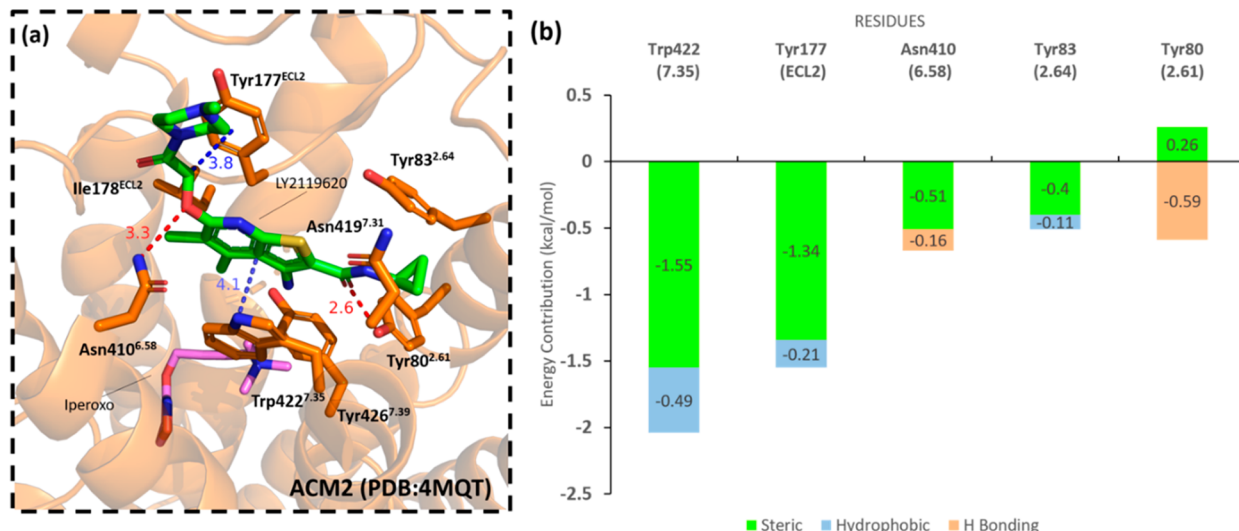


Figure 3. Detailed interaction and energy contribution of LY2119620 (green) in the allosteric binding pocket (Site A) of ACM2. The (a) interaction pattern and (b) energy contribution between LY2119620 and ACM2. Iperoxo (purple) is an orthosteric ligand.

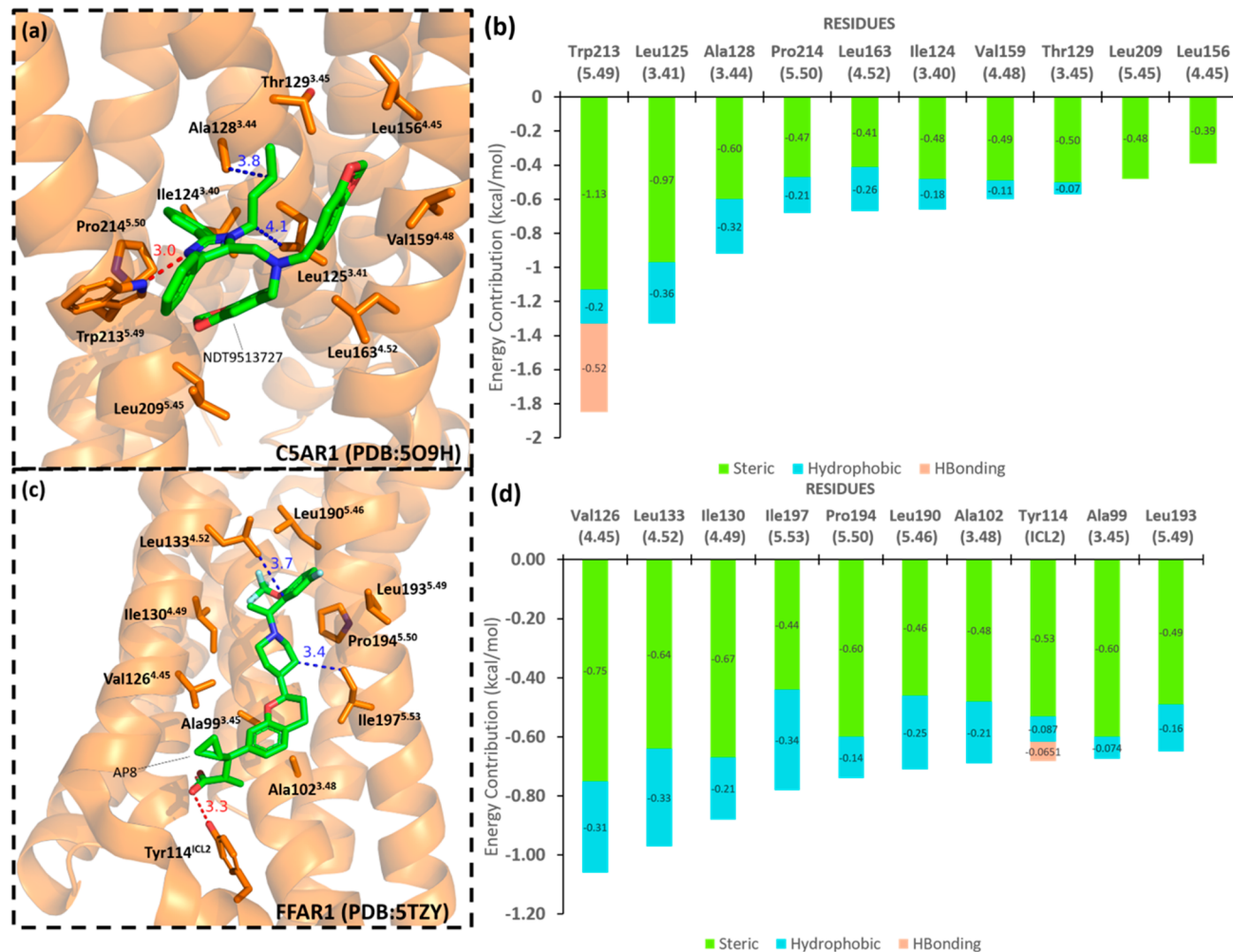


Figure 4. Detailed interaction and energy contribution of allosteric modulators in respective allosteric binding pockets (Site B). The (a) interaction pattern and (b) energy contribution between NDT9513727 and CSAR1. The (c) interaction pattern and (d) energy contribution between AP8 and FFAR1.

Table 3. Conserved Residues Involved in Site C

	2.39	2.40	2.43	6.36	7.53	8.47	8.48	8.49	8.50
ADRB2	T68	N69	I72	T274	Y326	S329	P330	D331	F332
DRD2	T69	N70	I73	M374	Y426	N430	I431	E432	F433
DRD3	T64	N65	V68	M330	Y383	N387	I388	E389	F390
DRD4	T69	N70	I73	V395	Y448	N452	A453	E454	F455
ACM1	N60	N61	L64	T366	Y418	N422	K423	A424	F425
ACM2	N58	N59	L62	T388	Y440	N444	A445	T446	F447
ACM4	N67	N68	L71	T401	Y453	N457	A458	T459	F460
AA1R	T44	F45	I48	S235	Y288	I292	Q293	K294	F295
AA2AR	T41	N42	V45	S234	Y288	I292	R293	E294	F295
P2RY1	I86	S87	M90	L261	Y324	G328	D329	T330	F331
CCR2	T77	D78	L81	V244	Y305	G309	E310	K311	F312
CCR5	T65	D66	L69	L236	Y297	G301	E302	K303	F304
CCR9	T83	D84	L87	V255	Y317	G321	E322	R323	F324
SHT1B	A84	N85	I88	T315	Y369	N373	E374	D375	F376
SHT2A	T109	N110	L113	V324	Y380	N384	K385	T386	Y387
OPRD	T84	N85	I86	M262	Y318	D322	E323	N324	F325
OPRK	T94	N95	I98	L275	Y330	D334	E335	N336	F337
CXCR4	T73	D74	R77	T240	Y302	G306	A307	K308	F309
CB1	S152	Y153	I156	T344	Y397	S401	K402	D403	L404
CB2	S69	Y70	I73	T246	Y299	S303	G304	E305	I306

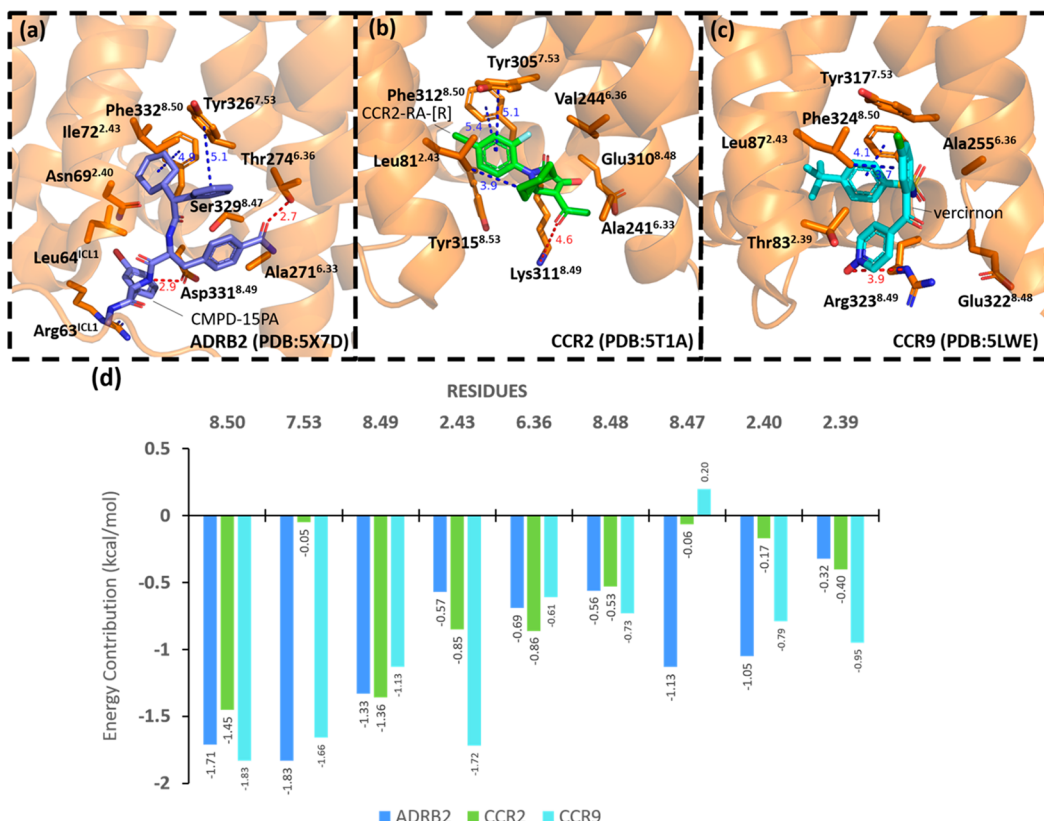


Figure 5. Detailed interaction and energy contribution of allosteric modulators in respective allosteric binding pockets (Site C). The interaction pattern between (a) CMPD-1SPA and ADRB2, (b) CCR2-RA-[R] and CCR2, (c) vercirnon and CCR9, and (d) the summarized energy contributions.

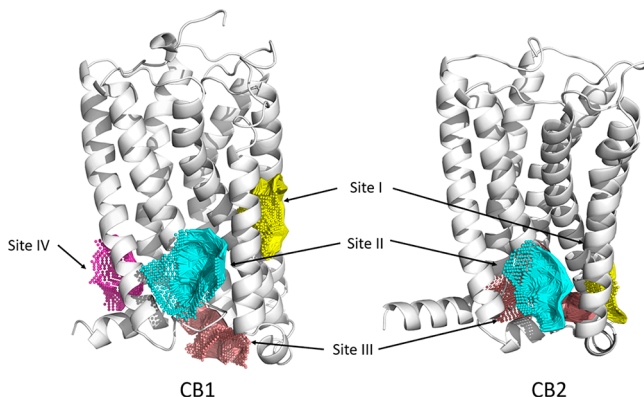


Figure 6. Predicted allosteric binding pocket of CB1 and CB2. There are four predicted allosteric binding pockets for CB1 and three for CB2. Three similar binding pockets are shared among the two receptors.

Tyr80^{2.61} contribute greatly to the binding of LY2119620 in ACM2. Although the distance between Trp422^{7.35} and LY2119620 is 4.1 Å, it contributes the greatest energy with a total energy contribution of -2.04 kcal/mol. Tyr177^{ECL2} contributes -1.55 kcal/mol to the binding of LY2119620. The energy sources for Trp422^{7.35} and Tyr177^{ECL2} are steric and hydrophobic interactions. With a distance of 2.6 Å, Tyr80^{2.61} forms a strong hydrogen bonding (H Bonding energy: -0.59 kcal/mol) with LY2119620 with a strong repulsion interaction (steric energy: 0.26 kcal/mol). Other residues including Asn410^{6.58} and Tyr83^{2.64} contribute -0.67 and -0.51 kcal/mol to the binding of LY2119620 in ACM2.

As shown in Figure 2, allosteric Site B locates near the TM4/5 region outside the 7TM domains. C5a anaphylatoxin

chemotactic receptor 1 (C5AR1) and the free fatty acid receptor 1 (FFAR1) are two GPCRs with a Site B allosteric pocket. The results calculated by MCCS for these two proteins are illustrated in Figure 4. Although this binding site has great diversity in binding behavior, several residues including 4.45, 4.52, and 5.50 at both proteins form strong steric or hydrophobic interactions with the allosteric modulators. However, they have different energy contribution patterns. For the complex of C5AR1-NDT9513727 (PDB: 5O9H),²⁰ Trp212^{5.49} contributes the greatest to the total binding energy (-1.85 kcal/mol) and forms strong hydrogen bonds with the modulator. Leu125^{3.41} and Ala128^{3.44} contribute to the binding of NDT9513727 with -1.33 and -0.92 kcal/mol. Other important residues including Pro214^{5.50}, Leu163^{4.52}, Ile124^{3.40}, Val159^{4.48}, and Thr129^{3.45} form hydrophobic interactions with NDT9513727. As to FFAR1,²¹ three conserved residues (Val126^{4.45}, Leu133^{4.52}, and Pro194^{5.50}) contribute to the binding of the allosteric modulator (AP8) with -1.06, -0.97, and -0.74 kcal/mol, respectively. The energy contributions of Ile130^{4.49} and Ile197^{5.53} are -0.88 and -0.78 kcal/mol, respectively.

As shown in Figure 2, Site C locates within the helical bundle of the receptor but was open to the cytoplasm and spatially overlapped with the G-protein binding site. The important residues in this binding pocket include 2.39, 2.40, 2.43, 6.36, 7.53, 8.47, 8.48, 8.49, and 8.50. Among these residues, 8.50 and 7.53 are highly conserved among all the class A GPCRs (Table 3). The three reported ligands share some similarities when binding with their respective receptors. We summarized the binding poses with ligand binding at this allosteric binding site on the basis of the three available PDB files (Figure 5a–c). A comparison of the energy contribution of each residue is shown in Figure 5d. Among the highest energy contribution residues,

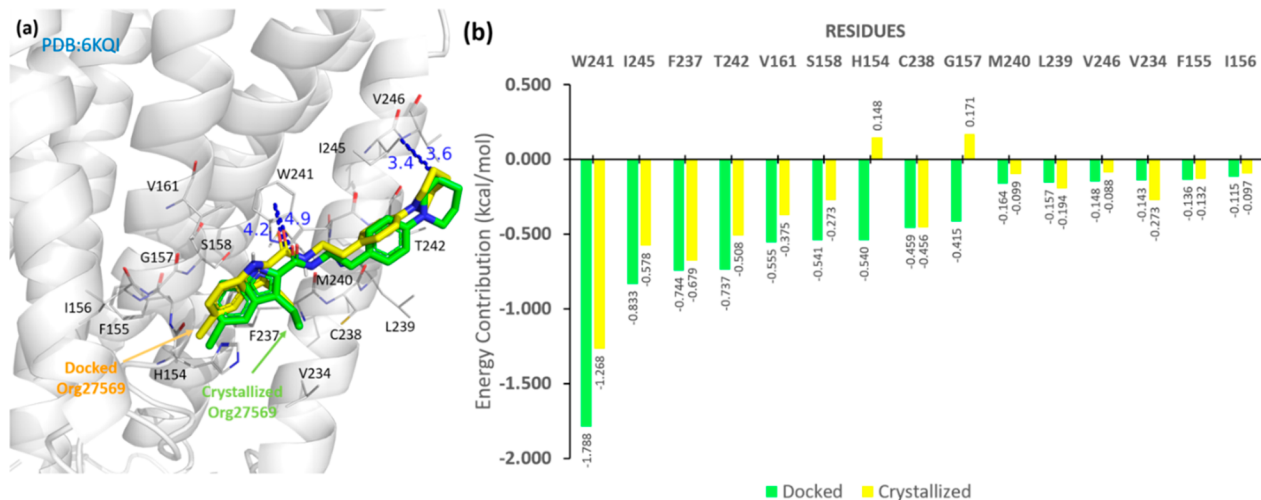


Figure 7. Alignment of crystallized and docked Org27569 and the residue energy contribution of key residues involved in the allosteric binding site in CB1. (a) Comparison of docking pose of Org27569 and cocrystallized Org27569 in CB1. (b) Residue energy contribution of key residue for the crystal structure of CB1-Org27569.

Table 4. Allosteric Modulators of CB1^{51–57}

Name	Effect	LogP	Structure	Reference
Org27569	NAM	5.27		⁵¹
GAT211	PAM	5.03		⁵²
ZCZ011	PAM	5.184		⁵³
RTI-371	PAM	5.64		⁵⁴
Cannabidiol	NAM	5.91		⁵⁵
Pregnenolone	NAM	3.98		⁵⁶
Fenofibrate	NAM	4.75		⁵⁷

F8.50 and D/K/R8.49 can form hydrophobic interactions or hydrogen bonds with all three reported modulators. As for 7.53, hydrophobic interactions can be observed for CMPD-15PA²² and CCR2-RA-[R]²³ but not for verciron.²⁴ The absence of the hydrophobic interaction is probably due to the near vertical spatial relationship between the residue and the benzene ring of verciron.

CB1 Reported Allosteric Site and CB2 Predicted Allosteric Binding Pocket. We applied several algorithms including CavityPlus (<http://www.pkumdl.cn:8000/cavityplus/>)

[index.php](#)),²⁵ PARS (<http://bioinf.uab.cat/cgi-bin/pars-cgi/pars.pl>),²⁶ and Sybyl to identify the potential allosteric binding pockets for both CB1 and CB2. CB1 and CB2 are highly similar in both sequence and structure. After collecting all possible cavities, we excluded cavities with poor ligability, druggability, or less motion correlation with known orthosteric sites. Finally, four sites on CB1 and three sites on CB2 can be observed as shown in Figure 6. Recently, the crystal structure of CB1 complexed with the negative allosteric modulator (NAM) Org27569

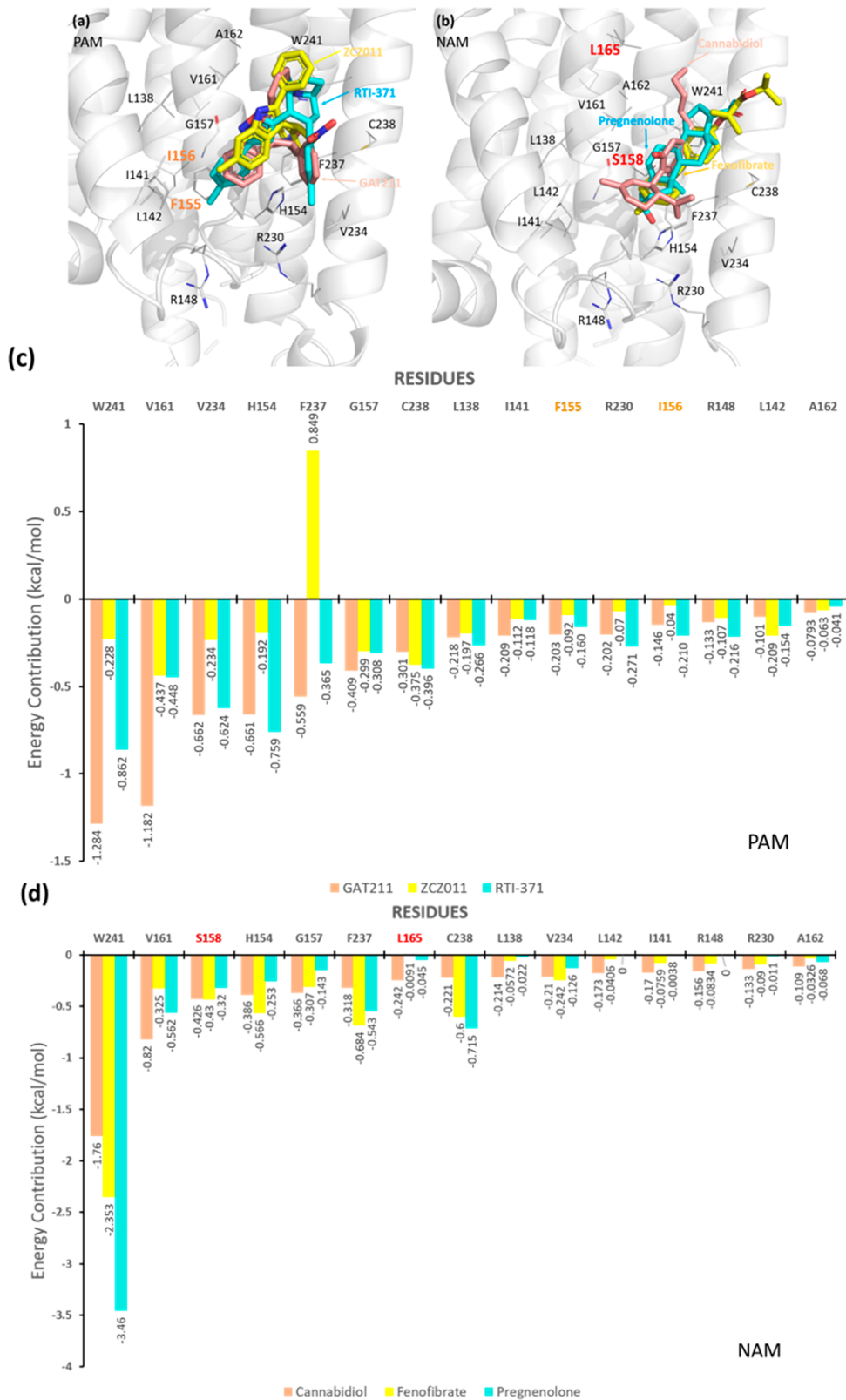


Figure 8. Detail interaction and energy decomposition of PAMs and NAMs with CB1. (a) Docking poses of CB1 PAMs, including GAT211, ZCZ011, and RTI-371. (b) Docking poses of CB1 NAMs, including CBD, Fenofibrate, and Pregnenolone. (c) Residue energy contribution of key residues for CB1 PAMs. (d) Residue energy contribution of key residues for CB1 NAMs.

and the agonist CP55940 has been reported²⁷ and revealed a novel extrahelical site that is within the inner leaflet of the cell membrane, which is the predicted Site II pocket in Figure 6.

Most of the literature reported that CB1 and CB2 should be similar in allosteric regulation mode. For example, cannabidiol (CBD) is reported as an allosteric modulator of CB1,²⁸ while some studies suggested that CBD also regulates CB2 in an

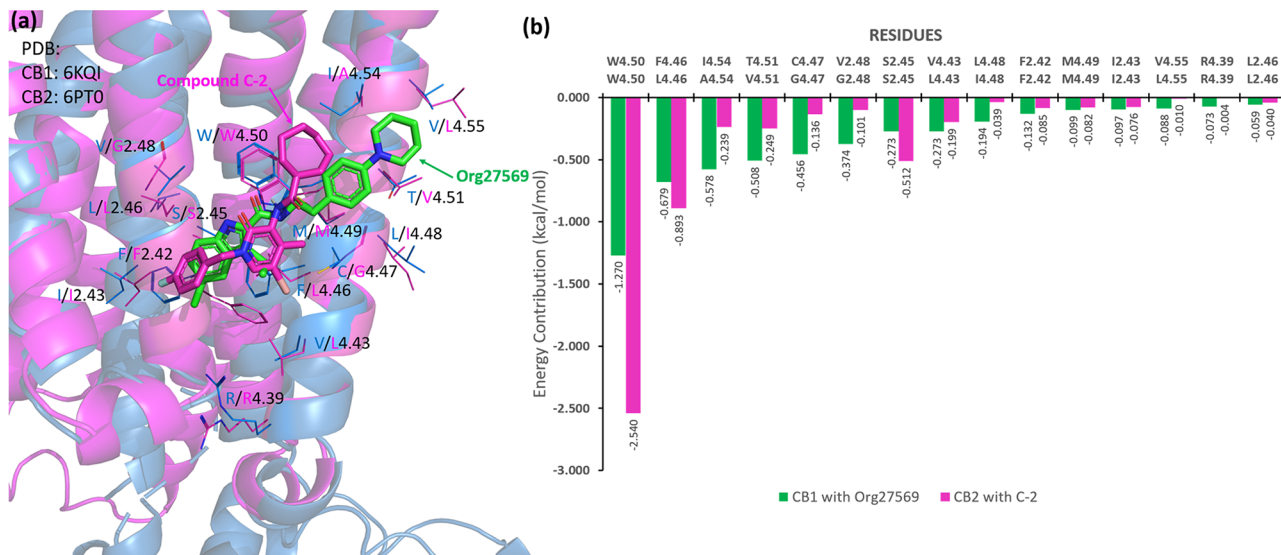


Figure 9. Comparison of docking poses and residue energy contribution between CB1/CB2 and their modulators. (a) Comparison of docking pose of modulators between CB1 and CB2. (b) Residue energy contribution of key residues between CB1 and CB2.

allosteric manner,²⁹ pepcan-12 can allosterically regulate both CB1³⁰ and CB2;³¹ Ec2la (or C-2), a newly developed CB2 synthetic modulator, is reported to positively affect the binding of CB1 with its agonist;³² etc. Therefore, we propose that CB2 may possess a similar allosteric binding region as CB1. In order to further study the recognition pattern involved in the allosteric binding site, we performed both the docking studies and/or molecular dynamic simulation in the following sections.

Detailed Binding Pattern for CB1 and Its Allosteric Modulators. Org27569 was first docked back to its reported allosteric binding site (Site II), as shown in Figure 7. The root-mean-square deviation (RMSD) between the docked pose and the cocrystallized one is 0.664 Å, which demonstrated the reliability of this docking method. By analyzing the residue energy contribution, we found that several residues may contribute to the recognition of allosteric modulators in CB1. For example, Trp241^{4,50} can form a strong hydrophobic interaction with Org27569, which is responsible for the majority of small-molecule modulators recognition in this binding site. Besides Trp241^{4,50}, other key residues including Phe237^{4,46}, His154^{2,41}, Cys238^{4,47}, Ser158^{2,45}, and Val161^{2,48} (shown in Figure 7) also contribute to the binding conformation of the Org27569.

In order to further investigate the allosteric binding pocket and key allosteric binding residues, we docked six allosteric modulators (Table 4) into CB1, including GAT211, ZCZ011, RTI-371, CBD, Fenofibrate, and Pregnenolone. Surprisingly, after analyzing the docking study with residue energy contribution shown in Figure 8, a clear and consistent binding mode can be observed for the known PAMs or NAMs. We found that the structures of PAMs can extend deeply into the middle of TM1 and TM2 and most of PAMs can form interactions with Phe155^{2,42} and Ile156^{2,43}, which are highlighted in Figure 8a, while Ser158^{2,45}, highlighted in Figure 8b, contributes greatly to the binding of NAMs. Interestingly, we found the energy contribution of Phe237^{4,46} was a positive value, which attributes to the repulsion of this residue.

Predicted Interactions between CB2 and Its Allosteric Modulator. To date, Ec2la (or C-2)³² is the only reported CB2 allosteric small-molecular modulator. On the basis of the previous binding pattern we summarized from CB1 and its allosteric modulators, we docked Ec2la to our reported CB2

cryo-EM structure⁹ and compared it with CB1-Org27569, as shown in Figure 9. Our results showed that their recognition pattern shared substantial similarities. Specially, three residues including W/W4.50, F/L4.46, and S/S2.45 contribute greater to the binding of CB2 than that of CB1. The difference in modulator interaction between CB1 and CB2 mostly resulted from the variation of residues involved in this region. Those residue variations may provide insight for the future development of novel allosteric modulators with high CB1/CB2 selectivity to achieve specificity and fewer side effects.

To further validate the binding pose of Ec2la in CB2, we performed ~134 ns MD simulation for the system of CB2-WIN complexed with Ec2la (or C-2) allosteric modulator (Figure 10c,d) and ~124 ns MD simulation for the complex of CB2-WIN without Ec2la modulator (Figure 10e). The RMSD values of CB2, Ec2la, and WIN compounds kept stable during the MD simulations, indicating that either 124 or 134 ns MD simulation is reasonable for predicting the dynamic behavior of CB2. Importantly, our results showed that Ec2la maintained stable interactions in the predicted allosteric binding site, indicating that this binding pose may be reliable. More information can be found in Figure 10.

CONCLUSION

Despite the high similarity of 7TMs and ligand binding pocket of class A GPCRs, their allosteric modulators can function in very distinct modes. In the present study, we applied our newly developed MCCS program to systematically analyze and characterize the known allosteric binding pockets of class A GPCRs. Furthermore, on the basis of the results from MCCS, we reported the detailed interactions and recognition pattern for CB1 NAMs or PAMs. Finally, we also predicted the potential allosteric binding site of CB2 and detailed interaction between CB2 and its modulator by MCCS and MD simulations. In summary, our MCCS program can quantitatively analyze the recognition and interaction patterns of small-molecule modulators to receptor proteins by characterizing the binding regions.

METHODS

Protein–Ligand Complexes. The X-ray crystal and cryo-EM structures were collected from Protein Data Bank <https://www.rcsb.org>³³ and

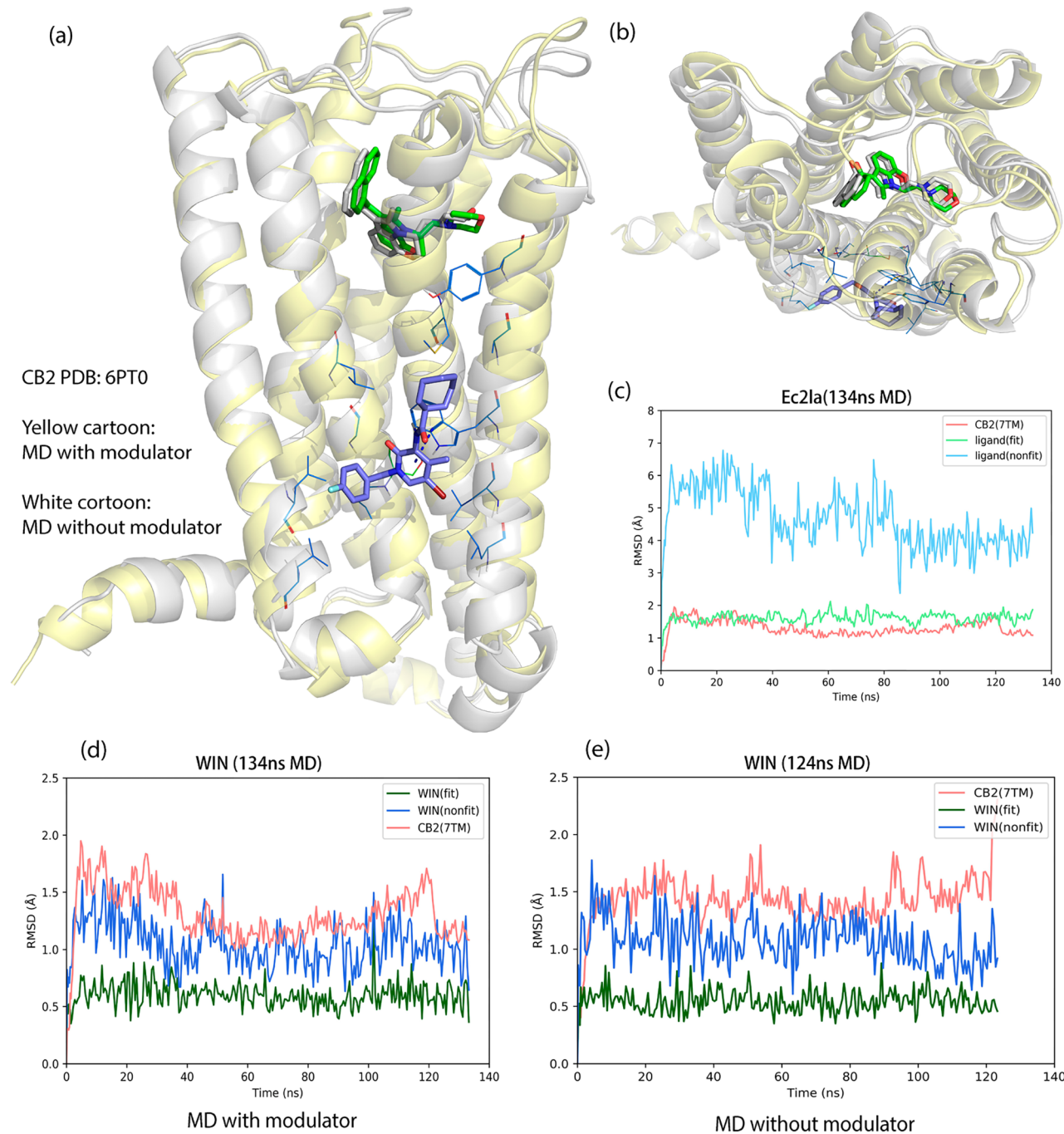


Figure 10. MD simulation between Ec2la (or C-2) and CB2 in predicted allosteric Site II. (a and b) Overlay of the whole system between pre-MD and post-MD. (c–e) RMSD of CB2, Ec2la, and WIN 55,212-2 during MD simulation.

GPCRs database <https://www.gpcrdb.org>.³⁴ Then, manual filtering, residue renumbering, and redundant chains/ions removal were performed with the help of our established utility programs to ensure the accuracy and quality of input data for MCCS.

CB1/CB2 Pocket Prediction and Analysis. Allosteric binding pockets of CB1/CB2 were predicted by CavityPlus Server (<http://www.pkumdl.cn:8000/cavityplus/index.php>),²⁵ Protein Allosteric and Regulatory Sites (PARS) (<http://bioinf.uab.cat/cgi-bin/pars-cgi/pars.pl>),²⁶ and Sybyl-X. All predicted pockets from these methods underwent further pocket analysis by CavityPlus Server. The ligandability, druggability, CavityScore, and the correction with the motions of orthosteric sites were taken into account when screening the possible allosteric pocket. The ligandability value represents the possibility of designing small ligands with high binding affinities to a certain cavity,

and the druggability value reflects the possibility of a cavity being a good target for binding drug-like molecules. The CavityScore is influenced by cavity volume, pocket lip size, hydrophobic volume, cavity surface area, and hydrogen-bond-forming surface area. The use of correction with the motions of orthosteric sites was based on the hypothesis that the motions of orthosteric and allosteric sites are highly correlated, and the Gaussian network model, a minimalist Normal-Mode Analysis model, was used to calculate the correlation. The correlations were normalized using the Z-score.

MCCS. The entire MCCS⁹ workflow was applied to our collected and prepared protein structures. Initially, each input PDB structure was split into a receptor PDB and a ligand PDB. A sequence of operations was carried out on the split PDBs. For the receptor, Chimera (Version 1.13.1)¹⁶ was first applied to repair the residues

with an incomplete side chain. Briefly, Chimera first scanned all the residues in a target protein and reported the residues with incomplete side chains; then, Chimera replaced each truncated side chain with a complete side chain of the same residue type using Dunbrack rotamer library.³⁵ For the ligand, PROPKA (version 3.1)¹⁸ was used to predict the corresponding pK_a values so as to determine whether the tertiary (3°) amide of the small molecule should be protonated. Then, using VEGA,¹⁷ polar hydrogens were added, Vina force fields and Gasteiger charges were applied, and the file format was transformed into PDBQT for both PDBs. Especially for the ligand PDB, torsions were defined by VEGA prior to the transformation into PDBQT. The output PDBQT files and the pK_a file of the ligand form the input of the next step in MCCS, jdock.

Jdock is a variant and successor of idock³⁶ built for MCCS. It adopts the same 5-term scoring function invented by AutoDock Vina¹⁷ and could generate a vector of residual free energy from the conformation either predicted from Monte Carlo-based docking algorithm or determined by X-ray crystallography or cryo-EM. In our experiment, the "score only" mode in jdock was used to directly compute the residue energy vector for the characterization of the three known allosteric binding pockets and applied docking with scoring mode for CB1/2 modulators within the predicted binding cavity.

Molecular Dynamics (MD) Simulation and Molecular Mechanics/Generalized Born Surface Area (MM/GBSA) Calculation. The system of Ec2la-CB2-WIN 55,212-2 complex (PDB ID: 6PT0)⁹ was used to perform the MD simulation. This system was put into a 0.15 M NaCl solution with a cubic water box and POPC lipid molecules. The same force fields or parameters^{37–39} described in our previous publications^{40–43} were applied to the CB2 receptor, water molecules (TIP3P model), and small molecule. MD simulation was carried out using the AMBER18⁴⁴ software package. The MD system was first relaxed by a set of minimizations by removing possible steric clashes. There were three phases for the subsequent NPT (constant particle number, pressure, and temperature) MD simulations: the relaxation phase (0.2 ns for each temperature from 50 to 250 K at a step of 50 K), the equilibrium phase (5 ns, 298 K), and the sampling phase (124 or 134 ns). The integration of the equations of motion was conducted at a time step of 1 fs for the relaxation phase and 2 fs for the equilibrium and sampling phases.

One hundred snapshots were evenly selected from the sampling phase for MM/GBSA binding free energy decomposition analysis. For each MD snapshot, the molecular mechanical (MM) energy (E_{MM}) and the MM/GBSA solvation free energy were calculated without further minimization.^{45,46} The interaction energies between each residue and ligand were calculated with the solvent effect being taken into account using a MM/GBSA solvation model.⁴⁷

AUTHOR INFORMATION

Corresponding Authors

Xiang-Qun Xie — Department of Pharmaceutical Sciences and Computational Chemical Genomics Screening Center, School of Pharmacy; National Center of Excellence for Computational Drug Abuse Research; Drug Discovery Institute; Departments of Computational Biology and Structural Biology, School of Medicine, University of Pittsburgh, Pittsburgh, Pennsylvania 15261, United States;  orcid.org/0000-0002-6881-6175; Email: xix15@pitt.edu

Authors

Zhiwei Feng — Department of Pharmaceutical Sciences and Computational Chemical Genomics Screening Center, School of Pharmacy; National Center of Excellence for Computational Drug Abuse Research, University of Pittsburgh, Pittsburgh, Pennsylvania 15261, United States;  orcid.org/0000-0001-6533-8932

Tianjian Liang — Department of Pharmaceutical Sciences and Computational Chemical Genomics Screening Center, School of Pharmacy; National Center of Excellence for Computational

Drug Abuse Research, University of Pittsburgh, Pittsburgh, Pennsylvania 15261, United States

Siyi Wang — Department of Pharmaceutical Sciences and Computational Chemical Genomics Screening Center, School of Pharmacy; National Center of Excellence for Computational Drug Abuse Research, University of Pittsburgh, Pittsburgh, Pennsylvania 15261, United States

Maozi Chen — Department of Pharmaceutical Sciences and Computational Chemical Genomics Screening Center, School of Pharmacy; National Center of Excellence for Computational Drug Abuse Research, University of Pittsburgh, Pittsburgh, Pennsylvania 15261, United States

Tianling Hou — Department of Pharmaceutical Sciences and Computational Chemical Genomics Screening Center, School of Pharmacy; National Center of Excellence for Computational Drug Abuse Research, University of Pittsburgh, Pittsburgh, Pennsylvania 15261, United States

Jack Zhao — Department of Pharmaceutical Sciences and Computational Chemical Genomics Screening Center, School of Pharmacy; National Center of Excellence for Computational Drug Abuse Research, University of Pittsburgh, Pittsburgh, Pennsylvania 15261, United States

Hui Chen — Department of Pharmaceutical Sciences and Computational Chemical Genomics Screening Center, School of Pharmacy; National Center of Excellence for Computational Drug Abuse Research, University of Pittsburgh, Pittsburgh, Pennsylvania 15261, United States

Yuehan Zhou — Department of Pharmaceutical Sciences and Computational Chemical Genomics Screening Center, School of Pharmacy; National Center of Excellence for Computational Drug Abuse Research, University of Pittsburgh, Pittsburgh, Pennsylvania 15261, United States

Complete contact information is available at:
<https://pubs.acs.org/10.1021/acschemneuro.0c00457>

Author Contributions

[§]Z.F., T.L., and S.W. contributed to this work equally. Z.F. and X.-Q.X. designed the project. M.C. designed and developed the MCCS algorithm. T.L., S.W., M.C., and Z.F. performed computational work, analyzed the data, and wrote the manuscript. All the authors reviewed the manuscript.

Notes

The authors declare no competing financial interest.

ACKNOWLEDGMENTS

The authors would like to acknowledge the funding support to the Xie laboratory from the NIH NIDA (P30 DA035778A1).

REFERENCES

- (1) Bockaert, J., and Philippe Pin, J. (1999) Molecular tinkering of G protein-coupled receptors: an evolutionary success. *EMBO J.* 18, 1723–1729.
- (2) Santos, R., Ursu, O., Gaulton, A., Bento, A. P., Donadi, R. S., Bologa, C. G., Karlsson, A., Al-Lazikani, B., Hersey, A., Oprea, T. I., and Overington, J. P. (2017) A comprehensive map of molecular drug targets. *Nat. Rev. Drug Discovery* 16, 19.
- (3) Liao, Z., Ju, Y., and Zou, Q. (2016) Prediction of G protein-coupled receptors with SVM-prot features and random forest. *Scientifica* 2016, 1.
- (4) Isberg, V., Mordalski, S., Munk, C., Rataj, K., Harpsøe, K., Hauser, A. S., Vroling, B., Bojarski, A. J., Vriend, G., and Gloriam, D. E. (2017) GPCRdb: an information system for G protein-coupled receptors. *Nucleic Acids Res.* 45, 2936.

- (5) Fredriksson, R., Lagerström, M. C., Lundin, L.-G., and Schiöth, H. B. (2003) The G-Protein-Coupled Receptors in the Human Genome Form Five Main Families. Phylogenetic Analysis, Paralogon Groups, and Fingerprints. *Mol. Pharmacol.* 63, 1256–1272.
- (6) Aizpurua-Olaizola, O., Elezgarai, I., Rico-Barrio, I., Zarandona, I., Etxebarria, N., and Usobiaga, A. (2017) Targeting the endocannabinoid system: future therapeutic strategies. *Drug Discovery Today* 22, 105–110.
- (7) Munro, S., Thomas, K. L., and Abu-Shaar, M. (1993) Molecular characterization of a peripheral receptor for cannabinoids. *Nature* 365, 61–65.
- (8) Wilson, R. I., and Nicoll, R. A. (2001) Endogenous cannabinoids mediate retrograde signalling at hippocampal synapses. *Nature* 410, 588–592.
- (9) Xing, C., Zhuang, Y., Xu, T. H., Feng, Z., Zhou, X. E., Chen, M., Wang, L., Meng, X., Xue, Y., Wang, J., Liu, H., McGuire, T. F., Zhao, G., Melcher, K., Zhang, C., Xu, H. E., and Xie, X. Q. (2020) Cryo-EM Structure of the Human Cannabinoid Receptor CB2-Gi Signaling Complex. *Cell* 180, 645–654.
- (10) Basu, S., Ray, A., and Dittel, B. N. (2011) Cannabinoid receptor 2 is critical for the homing and retention of marginal zone B lineage cells and for efficient T-independent immune responses. *J. Immunol.* 187, 5720–5732.
- (11) Feng, Z., Hu, G., Ma, S., and Xie, X.-Q. (2015) Computational Advances for the Development of Allosteric Modulators and Bitopic Ligands in G Protein-Coupled Receptors. *AAPS J.* 17, 1080–1095.
- (12) Tanaka, M., Yoshida, K., Fukuma, S., Ito, K., Matsushita, K., Fukagawa, M., Fukuhara, S., and Akizawa, T. (2016) Effects of Secondary Hyperparathyroidism Treatment on Improvement in Anemia: Results from the MBD-SD Study. *PLoS One* 11, No. e0164865.
- (13) Carter, N. J., and Keating, G. M. (2007) Maraviroc. *Drugs* 67, 2277–2288.
- (14) Bridges, T. M., and Lindsley, C. W. (2008) G-protein-coupled receptors: from classical modes of modulation to allosteric mechanisms. *ACS Chem. Biol.* 3, 530–541.
- (15) Lyu, J., Wang, S., Balus, T. E., Singh, I., Levit, A., Moroz, Y. S., O'Meara, M. J., Che, T., Algaas, E., Tolmachova, K., Tolmachev, A. A., Shoichet, B. K., Roth, B. L., and Irwin, J. J. (2019) Ultra-large library docking for discovering new chemotypes. *Nature* 566, 224–229.
- (16) Pettersen, E. F., Goddard, T. D., Huang, C. C., Couch, G. S., Greenblatt, D. M., Meng, E. C., and Ferrin, T. E. (2004) UCSF Chimera—a visualization system for exploratory research and analysis. *J. Comput. Chem.* 25, 1605–1612.
- (17) Pedretti, A., Villa, L., and Vistoli, G. (2004) VEGA—an open platform to develop chemo-bio-informatics applications, using plug-in architecture and script programming. *J. Comput.-Aided Mol. Des.* 18, 167–173.
- (18) Olsson, M. H., Søndergaard, C. R., Rostkowski, M., and Jensen, J. H. (2011) PROPKA3: consistent treatment of internal and surface residues in empirical pK_a predictions. *J. Chem. Theory Comput.* 7, 525–537 and computation.
- (19) Kruse, A. C., Ring, A. M., Manglik, A., Hu, J., Hu, K., Eitel, K., Hübner, H., Pardon, E., Valant, C., Sexton, P. M., Christopoulos, A., Felder, C. C., Gmeiner, P., Steyaert, J., Weis, W. I., Garcia, K. C., Wess, J., and Kobilka, B. K. (2013) Activation and allosteric modulation of a muscarinic acetylcholine receptor. *Nature* 504, 101–106.
- (20) Robertson, N., Rappas, M., Doré, A. S., Brown, J., Bottegoni, G., Koglin, M., Cansfield, J., Jazayeri, A., Cooke, R. M., and Marshall, F. H. (2018) Structure of the complement C5a receptor bound to the extra-helical antagonist NDT9513727. *Nature* 553, 111–114.
- (21) Lu, J., Byrne, N., Wang, J., Bricogne, G., Brown, F. K., Chobanian, H. R., Colletti, S. L., Di Salvo, J., Thomas-Fowlkes, B., Guo, Y., Hall, D. L., Hadix, J., Hastings, N. B., Hermes, J. D., Ho, T., Howard, A. D., Josien, H., Kornienko, M., Lumb, K. J., Miller, M. W., Patel, S. B., Pio, B., Plummer, C. W., Sherborne, B. S., Sheth, P., Souza, S., Tummala, S., Vonrhein, C., Webb, M., Allen, S. J., Johnston, J. M., Weinglass, A. B., Sharma, S., and Soisson, S. M. (2017) Structural basis for the cooperative allosteric activation of the free fatty acid receptor GPR40. *Nat. Struct. Mol. Biol.* 24, 570–577.
- (22) Liu, X., Ahn, S., Kahsai, A. W., Meng, K.-C., Latorraca, N. R., Pani, B., Venkatakrishnan, A. J., Masoudi, A., Weis, W. I., Dror, R. O., Chen, X., Lefkowitz, R. J., and Kobilka, B. K. (2017) Mechanism of intracellular allosteric β2AR antagonist revealed by X-ray crystal structure. *Nature* 548, 480–484.
- (23) Zheng, Y., Qin, L., Zacarias, N. V. O., de Vries, H., Han, G. W., Gustavsson, M., Dabros, M., Zhao, C., Cherney, R. J., Carter, P., Stamos, D., Abagyan, R., Cherezov, V., Stevens, R. C., Ijzerman, A. P., Heitman, L. H., Tebben, A., Kufareva, I., and Handel, T. M. (2016) Structure of CC chemokine receptor 2 with orthosteric and allosteric antagonists. *Nature* 540, 458–461.
- (24) Oswald, C., Rappas, M., Kean, J., Doré, A. S., Errey, J. C., Bennett, K., Deflorian, F., Christopher, J. A., Jazayeri, A., Mason, J. S., Congreve, M., Cooke, R. M., and Marshall, F. H. (2016) Intracellular allosteric antagonism of the CCR9 receptor. *Nature* 540, 462–465.
- (25) Xu, Y., Wang, S., Hu, Q., Gao, S., Ma, X., Zhang, W., Shen, Y., Chen, F., Lai, L., and Pei, J. (2018) CavityPlus: a web server for protein cavity detection with pharmacophore modelling, allosteric site identification and covalent ligand binding ability prediction. *Nucleic Acids Res.* 46, W374–W379.
- (26) Panjkovich, A., and Daura, X. (2014) PARS: a web server for the prediction of Protein Allosteric and Regulatory Sites. *Bioinformatics* 30, 1314–1315.
- (27) Shao, Z., Yan, W., Chapman, K., Ramesh, K., Ferrell, A. J., Yin, J., Wang, X., Xu, Q., and Rosenbaum, D. M. (2019) Structure of an allosteric modulator bound to the CB1 cannabinoid receptor. *Nat. Chem. Biol.* 15, 1199–1205.
- (28) Laprairie, R. B., Bagher, A. M., Kelly, M. E. M., and Denovan-Wright, E. M. (2015) Cannabidiol is a negative allosteric modulator of the cannabinoid CB1 receptor. *Br. J. Pharmacol.* 172, 4790–4805.
- (29) Tham, M., Yilmaz, O., Alaverdashvili, M., Kelly, M. E. M., Denovan-Wright, E. M., and Laprairie, R. B. (2019) Allosteric and orthosteric pharmacology of cannabidiol and cannabidiol-dimethylheptyl at the type 1 and type 2 cannabinoid receptors. *Br. J. Pharmacol.* 176, 1455–1469.
- (30) Bauer, M., Chicca, A., Tamborrini, M., Eisen, D., Lerner, R., Lutz, B., Poetz, O., Pluschke, G., and Gertsch, J. (2012) Identification and quantification of a new family of peptide endocannabinoids (Pepcans) showing negative allosteric modulation at CB1 receptors. *J. Biol. Chem.* 287, 36944–36967.
- (31) Petrucci, V., Chicca, A., Glasmacher, S., Paloczi, J., Cao, Z., Pacher, P., and Gertsch, J. (2017) Pepcan-12 (RVD-hemopressin) is a CB2 receptor positive allosteric modulator constitutively secreted by adrenals and in liver upon tissue damage. *Sci. Rep.* 7, 9560.
- (32) Gado, F., Di Cesare Mannelli, L., Lucarini, E., Bertini, S., Cappelli, E., Digiocomo, M., Stevenson, L. A., Macchia, M., Tuccinardi, T., Ghelardini, C., Pertwee, R. G., and Manera, C. (2019) Identification of the First Synthetic Allosteric Modulator of the CB2 Receptors and Evidence of Its Efficacy for Neuropathic Pain Relief. *J. Med. Chem.* 62, 276–287.
- (33) Berman, H. M., Bourne, P. E., Westbrook, J., and Zardecki, C. (2003) The protein data bank. *Protein Structure: Determination, Analysis, and Applications for Drug Discovery*, pp 394–410, CRC Press.
- (34) Pády-Szekeres, G., Munk, C., Tsionkov, T. M., Mordalski, S., Harpsøe, K., Hauser, A. S., Bojarski, A. J., and Gloriam, D. E. (2018) GPCRdb in 2018: adding GPCR structure models and ligands. *Nucleic Acids Res.* 46, D440–D446.
- (35) Shapovalov, M. V., and Dunbrack, R. L., Jr. (2011) A smoothed backbone-dependent rotamer library for proteins derived from adaptive kernel density estimates and regressions. *Structure* 19, 844–858.
- (36) Li, H., Leung, K.-S., and Wong, M.-H. (2012) idock: A multithreaded virtual screening tool for flexible ligand docking. *IEEE Symposium on Computational Intelligence in Bioinformatics and Computational Biology (CIBCB)* 2012, 77–84.

- (37) Dickson, C. J., Madej, B. D., Skjevik, A. A., Betz, R. M., Teigen, K., Gould, I. R., and Walker, R. C. (2014) Lipid14: The Amber Lipid Force Field. *J. Chem. Theory Comput.* 10, 865–879.
- (38) Maier, J. A., Martinez, C., Kasavajhala, K., Wickstrom, L., Hauser, K. E., and Simmerling, C. (2015) ff14SB: Improving the Accuracy of Protein Side Chain and Backbone Parameters from ff99SB. *J. Chem. Theory Comput.* 11, 3696–3713.
- (39) Wang, J. M., Wolf, R. M., Caldwell, J. W., Kollman, P. A., and Case, D. A. (2004) Development and testing of a general amber force field. *J. Comput. Chem.* 25, 1157–1174.
- (40) Cheng, J., Wang, S., Lin, W., Wu, N., Wang, Y., Chen, M., Xie, X.-Q., and Feng, Z. (2019) Computational Systems Pharmacology-Target Mapping for Fentanyl-laced Cocaine Overdose. *ACS Chem. Neurosci.* 10, 3486–3499.
- (41) Wu, N., Feng, Z., He, X., Kwon, W., Wang, J., and Xie, X.-Q. (2019) Insight of Captagon Abuse by Chemogenomics Knowledge-base-guided Systems Pharmacology Target Mapping Analyses. *Sci. Rep.* 9, 2268.
- (42) Chen, M., Jing, Y., Wang, L., Feng, Z., and Xie, X.-Q. (2019) DAKB-GPCRs: An Integrated Computational Platform for Drug Abuse Related GPCRs. *J. Chem. Inf. Model.* 59, 1283–1289.
- (43) Wang, Y., Lin, W., Wu, N., He, X., Wang, J., Feng, Z., and Xie, X.-Q. (2018) An insight into paracetamol and its metabolites using molecular docking and molecular dynamics simulation. *J. Mol. Model.* 24, 243.
- (44) Case, D. A., Ben-Shalom, I. Y., Brozell, S. R., Cerutti, D. S., Cheatham, I. T. E., Cruzeiro, V. W. D., Darden, T. A., Duke, R. E., Ghoreishi, D., Gilson, M. K., Gohlke, H., Goetz, A. W., Greene, D., Harris, R., Homeyer, N., Izadi, S., Kovalenko, A., Kurtzman, T., Lee, T. S., LeGrand, S., Li, P., Lin, C., Liu, J., Luchko, T., Luo, R., Mermelstein, D. J., Merz, K. M., Miao, Y., Monard, G., Nguyen, C., Nguyen, H., Omelyan, I., Onufriev, A., Pan, F., Qi, R., Roe, D. R., Roitberg, A., Sagui, C., Schott-Verdugo, S., Shen, J., Simmerling, C. L., Smith, J., Salomon-Ferrer, R., Swails, J., Walker, R. C., Wang, J., Wei, H., Wolf, R. M., Wu, X., Xiao, L. D. M. Y., and Kollman, P. A. (2018) AMBER 2018, University of California, San Francisco.
- (45) Hou, T., Wang, J., Li, Y., and Wang, W. (2011) Assessing the performance of the MM/PBSA and MM/GBSA methods. I. The accuracy of binding free energy calculations based on molecular dynamics simulations. *J. Chem. Inf. Model.* 51, 69–82.
- (46) Hou, T., Wang, J., Li, Y., and Wang, W. (2011) Assessing the performance of the molecular mechanics/Poisson Boltzmann surface area and molecular mechanics/generalized Born surface area methods. II. The accuracy of ranking poses generated from docking. *J. Comput. Chem.* 32, 866–877.
- (47) Hawkins, G. D., Cramer, C. J., and Truhlar, D. G. (1996) Parametrized models of aqueous free energies of solvation based on pairwise descreening of solute atomic charges from a dielectric medium. *J. Phys. Chem.* 100, 19824–19839.
- (48) Cheng, R. K. Y., Fiez-Vandal, C., Schlenker, O., Edman, K., Aggeler, B., Brown, D. G., Brown, G. A., Cooke, R. M., Dumelin, C. E., Doré, A. S., Geschwindner, S., Grebner, C., Hermansson, N.-O., Jazayeri, A., Johansson, P., Leong, L., Prihandoko, R., Rappas, M., Soutter, H., Snijder, A., Sundström, L., Tehan, B., Thornton, P., Troast, D., Wiggin, G., Zhukov, A., Marshall, F. H., and Dekker, N. (2017) Structural insight into allosteric modulation of protease-activated receptor 2. *Nature* 545, 112–115.
- (49) Srivastava, A., Yano, J., Hirozane, Y., Kefala, G., Gruswitz, F., Snell, G., Lane, W., Ivetac, A., Aertgeerts, K., Nguyen, J., Jennings, A., and Okada, K. (2014) High-resolution structure of the human GPR40 receptor bound to allosteric agonist TAK-875. *Nature* 513, 124–127.
- (50) Zhang, D., Gao, Z.-G., Zhang, K., Kiselev, E., Crane, S., Wang, J., Paolella, S., Yi, C., Ma, L., Zhang, W., Han, G. W., Liu, H., Cherezov, V., Katritch, V., Jiang, H., Stevens, R. C., Jacobson, K. A., Zhao, Q., and Wu, B. (2015) Two disparate ligand-binding sites in the human P2Y1 receptor. *Nature* 520, 317–321.
- (51) Price, M. R., Baillie, G. L., Thomas, A., Stevenson, L. A., Easson, M., Goodwin, R., McLean, A., McIntosh, L., Goodwin, G., Walker, G., Westwood, P., Marrs, J., Thomson, F., Cowley, P., Christopoulos, A., Pertwee, R. G., and Ross, R. A. (2005) Allosteric Modulation of the Cannabinoid CB₁ Receptor. *Mol. Pharmacol.* 68, 1484–1495.
- (52) Laprairie, R. B., Kulkarni, P. M., Deschamps, J. R., Kelly, M. E. M., Janero, D. R., Cascio, M. G., Stevenson, L. A., Pertwee, R. G., Kenakin, T. P., Denovan-Wright, E. M., and Thakur, G. A. (2017) Enantiospecific Allosteric Modulation of Cannabinoid 1 Receptor. *ACS Chem. Neurosci.* 8, 1188–1203.
- (53) Ignatowska-Jankowska, B. M., Baillie, G. L., Kinsey, S., Crowe, M., Ghosh, S., Owens, R. A., Damaj, I. M., Poklis, J., Wiley, J. L., Zanda, M., Zanato, C., Greig, I. R., Lichtman, A. H., and Ross, R. A. (2015) A Cannabinoid CB1 Receptor-Positive Allosteric Modulator Reduces Neuropathic Pain in the Mouse with No Psychoactive Effects. *Neuropsychopharmacology* 40, 2948–2959.
- (54) Navarro, H. A., Howard, J. L., Pollard, G. T., and Carroll, F. I. (2009) Positive allosteric modulation of the human cannabinoid (CB1) receptor by RTI-371, a selective inhibitor of the dopamine transporter. *Br. J. Pharmacol.* 156, 1178–1184.
- (55) Laprairie, R. B., Bagher, A. M., Kelly, M. E. M., and Denovan-Wright, E. M. (2015) Cannabidiol is a negative allosteric modulator of the cannabinoid CB1 receptor. *Br. J. Pharmacol.* 172, 4790–4805.
- (56) Vallée, M., Vitiello, S., Bellocchio, L., Hébert-Chatalain, E., Monlezun, S., Martin-Garcia, E., Kasanetz, F., Baillie, G. L., Panin, F., Cathala, A., Roullot-Lacarrière, V., Fabre, S., Hurst, D. P., Lynch, D. L., Shore, D. M., Deroche-Gamonet, V., Spampinato, U., Revest, J.-M., Maldonado, R., Reggio, P. H., Ross, R. A., Marsicano, G., and Piazza, P. V. (2014) Pregnenolone Can Protect the Brain from Cannabis Intoxication. *Science* 343, 94–98.
- (57) Priestley, R. S., Nickolls, S. A., Alexander, S. P. H., and Kendall, D. A. (2015) A potential role for cannabinoid receptors in the therapeutic action of fenofibrate. *FASEB J.* 29, 1446–1455.